Nečas Center for Mathematical Modeling

Anisotropic hp-adaptive method based on interpolation error estimates in the H^1-seminorm

V. Dolejší

Preprint no. 2015-11

http://ncmm.karlin.mff.cuni.cz/

Anisotropic hp-adaptive method based on interpolation error estimates in the H^1-seminorm

Vít Dolejší

Cordially dedicated to prof. Ivo Babuška, the founder of *hp*-methods

Abstract

We develop a new technique which, for the given smooth function, generates the anisotropic triangular grid and the corresponding polynomial approximation degrees based on the minimization of the interpolation error in the broken H^1-seminorm. This technique can be employed for the numerical solution of boundary value problems with the aid of finite element methods. We present the theoretical background of this approach and show several numerical examples demonstrating the efficiency of the proposed anisotropic adaptive strategy in comparison with other adaptive approaches.

[1]

Keywords: *hp*-methods, anisotropic mesh adaptation, interpolation error estimates
MSC 2010: 65N50, 65N15, 65D05

1 Introduction

An automatic mesh adaptation is an efficient tool for the numerical solution of partial differential equations (PDEs). In this paper we develop the method which combines two approaches:

- *(isotropic) hp-adaptive methods*, which allow the adaptation in the element size h as well as in the polynomial degree of approximation p. The origins of the *hp*-methods, which give *exponential rate* of the convergence, date back to the pioneering work of Ivo Babuška et al, see, e.g., [3, 8, 24, 25, 26, 28].
- *anisotropic mesh adaptation* techniques, generating anisotropic elements (i.e., long and thin triangles), which are suitable in computation of problems with boundary or internal layers, see, e.g., [1, 2, 9, 14, 16, 20, 21, 29].

The combination of both approaches offers enough flexibility in the choice of finite element spaces where an approximate solution is sought. This allows to achieve the prescribed error tolerance with significantly lower number of degrees of freedom than the standard numerical methods. The triangular grid with the corresponding polynomial approximation degrees is called the *anisotropic hp-mesh*.

In [13] we developed an adaptive technique, which constructs, for the given function $u : \Omega \to \mathbb{R}^2$, an anisotropic *hp*-mesh such that

(i) the *interpolation error* of a projection of u on $S_{h\mathsf{p}}$ (= space of discontinuous piecewise polynomial functions uniquely defined for each *hp*-mesh, cf. (3.1)) in the L^q-norm ($q \in [1, \infty]$) is below the given tolerance,

(ii) the dimension of $S_{h\mathsf{p}}$ (=*number of degrees of freedom*) is the smallest possible.

In this paper, we deal with a modified problem where the interpolation error in condition (i) is considered in the broken H^1-seminorm which is more natural particularly for the solution of second order boundary value problems. In [13], we approximated the interpolation error by a polynomial function and derived its bound which was the basis of the optimization of the element shape. In this paper, we derive the approximation of the gradient of the interpolation error function together with its bound. Consequently,

[1] The research of V. Dolejší has been supported by the Grant No. 13-00522S of the Czech Science Foundation. The author acknowledges also the membership in the Nečas Center for Mathematical Modeling ncmm.karlin.mff.cuni.cz.

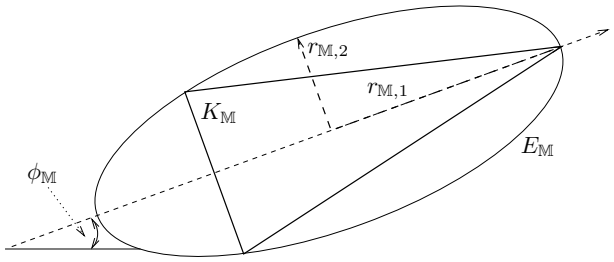

Fig. 1: The ellipse $E_{\mathbb{M}}$ with the length of semi-axes $r_{\mathbb{M},1}$, $r_{\mathbb{M},2}$ and the orientation $\phi_{\mathbb{M}}$, and the corresponding triangle $K_{\mathbb{M}}$ with the anisotropy $\{r_{\mathbb{M},1}, r_{\mathbb{M},1}/r_{\mathbb{M},2}, \phi_{\mathbb{M}}\}$.

we use the technique from [13] for the element shape optimization (cf. Theorem 3.1). Moreover, at the end of Section 3, we discuss a possible extension of this approach to the broken $W^{k,q}$-seminorm, where $q \in [1, \infty]$ and $k \geq 1$.

The content of the rest of the paper is the following. In Section 2, we introduce basic notations and properties of anisotropic *hp*-meshes. In Section 3 we present a theoretical background of the presented *hp*-adaptation algorithm employing some results from [13]. Its application to the numerical solution of boundary value problems is briefly given in Section 4. The resulting adaptive technique is independent of the considered problem and can be combined with conforming as well as nonconforming finite element approximations. The efficiency of the algorithm is demonstrated by experiments in Section 5. Finally, we add several concluding remarks.

2 Anisotropic *hp*-meshes

In this section we recall basic terms and definitions of the anisotropic *hp*-meshes, the details can be found in [13]. Let $\Omega \subset \mathbb{R}^2$ be a bounded computational domain with a polygonal boundary $\partial\Omega$. We denote by $\mathscr{T}_h = \{K\}$ $(h > 0)$ a conforming *triangulation* of Ω and by $\mathscr{F}_h$ the set of edges of $\mathscr{T}_h$. The edges $\boldsymbol{e} \in \mathscr{F}_h$ are considered as vectors from $\mathbb{R}^2$ given by its endpoints, the orientation of $\boldsymbol{e} \in \mathscr{F}_h$ is arbitrary.

2.1 Anisotropic triangle

The anisotropy of a triangle is described by a matrix $\mathbb{M} \in \mathrm{Sym}$, where Sym is the space of 2×2 symmetric positively definite matrices. Let the matrix $\mathbb{M} \in \mathrm{Sym}$ be given, it can be decomposed in the form

$$\mathbb{M} = \mathbb{Q}_{\phi_{\mathbb{M}}}^{\mathrm{T}} \mathrm{diag}\,(\lambda_{\mathbb{M},1}, \lambda_{\mathbb{M},2})\, \mathbb{Q}_{\phi_{\mathbb{M}}}, \tag{2.1}$$

where $\mathrm{diag}(a, b)$ denotes the diagonal matrix with the entries a and b, $0 < \lambda_{\mathbb{M},1} \leq \lambda_{\mathbb{M},2}$ are the eigenvalues of $\mathbb{M}$, $\phi_{\mathbb{M}} \in [0, \pi)$ and $\mathbb{Q}_\phi$ is the *rotation* about the angle ϕ in the counter clockwise direction. Moreover, the set

$$E_{\mathbb{M}} := \left\{ x \in \mathbb{R}^2;\ x^{\mathrm{T}} \mathbb{M} x \leq 1 \right\}, \tag{2.2}$$

defines an *ellipse* whose semi-axes have lengths $r_{\mathbb{M},i} = (\lambda_{\mathbb{M},i})^{-1/2}$, $i = 1, 2$ and its orientation is $\phi_{\mathbb{M}}$ (=angle between the major semi-axis and the axis x_1 of the coordinate system), see Figure 1.

Definition 2.1. *Let $\mathbb{M} \in \mathrm{Sym}$ and let $E_{\mathbb{M}}$ be the ellipse given by* (2.2)*. Let $K_{\mathbb{M}}$ be an acute-angle isosceles triangle which is inscribed into the ellipse $E_{\mathbb{M}}$ and which has the maximal possible area, see Figure 1. We call $K_{\mathbb{M}}$ the* triangle corresponding *to $\mathbb{M}$.*

Similarly as in [4, 5, 20, 21] and the works cited therein, we describe the anisotropy of a triangle by three parameters: the *size*, the *aspect ratio* and the *orientation*.

Definition 2.2. *Let $K_{\mathbb{M}}$ be the triangle corresponding to $\mathbb{M} \in \mathrm{Sym}$ and $\lambda_{\mathbb{M},1}$, $\lambda_{\mathbb{M},2}$ and $\phi_{\mathbb{M}}$ be given by* (2.1)*. Let $r_{\mathbb{M},i} = (\lambda_{\mathbb{M},i})^{-1/2}$, $i = 1, 2$ be the lengths of semi-axes of $E_{\mathbb{M}}$. We say that*

- *$r_{\mathbb{M},1}$ is the* size *of $K_{\mathbb{M}}$,*
- *$\sigma_{\mathbb{M}} := \frac{r_{\mathbb{M},1}}{r_{\mathbb{M},2}} \geq 1$ is the* aspect ratio *of $K_{\mathbb{M}}$,*

- $\phi_{\mathbb{M}}$ *is the* orientation *of* $K_{\mathbb{M}}$.

The triplet $\{r_{\mathbb{M},1}, \sigma_{\mathbb{M}}, \phi_{\mathbb{M}}\}$ *is called the* anisotropy *of* $K_{\mathbb{M}}$.

Obviously, the matrix $\mathbb{M} \in \mathrm{Sym}$ defines a Riemann metric in $\mathbb{R}^2$, where the distance of $x, y \in \mathbb{R}^2$ is given by $\|x-y\|_{\mathbb{M}} := \big((x-y)^{\mathrm{T}}\mathbb{M}(x-y)\big)^{1/2}$. For the purpose of the definition of an optimal *hp*-mesh, we recall one result from [9, Section 3], which implies that triangle $K_{\mathbb{M}}$ corresponding to $\mathbb{M}$ is equilateral in the metric given by $\mathbb{M}$.

Lemma 2.1. *Let* $\mathbb{M} \in \mathrm{Sym}$ *and* $K_{\mathbb{M}}$ *be the corresponding triangle. Let* $\boldsymbol{e}_i$, $i = 1, 2, 3$ *denote the edges of* $K_{\mathbb{M}}$*, which are considered as vectors from* $\mathbb{R}^2$ *given by their endpoints. Then*

$$\|\boldsymbol{e}_i\|_{\mathbb{M}} := \Big(\boldsymbol{e}_i^{\mathrm{T}}\mathbb{M}\boldsymbol{e}_i\Big)^{1/2} = \sqrt{3}, \quad i = 1, 2, 3. \tag{2.3}$$

2.2 Anisotropic meshes

Similarly as in, e.g., [2, 9, 14, 16, 22, 23], we define an anisotropic triangular grid $\mathscr{T}_h$ as a mesh consisting of equilateral triangles with respect to the given Riemann metric. Let $\mathcal{M} : \Omega \to \mathrm{Sym}$ be an integrable mapping. We define the distance between $\boldsymbol{v}_0 \in \Omega$ and $\boldsymbol{v}_1 \in \Omega$ by

$$\|\boldsymbol{v}_1 - \boldsymbol{v}_0\|_{\mathcal{M}} := \int_0^1 \Big((\boldsymbol{v}_1 - \boldsymbol{v}_0)^{\mathrm{T}}\mathcal{M}(\boldsymbol{v}_0 + t(\boldsymbol{v}_1 - \boldsymbol{v}_0))(\boldsymbol{v}_1 - \boldsymbol{v}_0)\Big)^{1/2} \mathrm{d}t,$$

which induces a metric on Ω. Thus, we call $\mathcal{M}$ the *Riemann metric* on Ω. In virtue of (2.3), it would be natural to define a mesh $\mathscr{T}_h$ such that

$$\|\boldsymbol{e}\|_{\mathcal{M}} = \sqrt{3} \quad \forall \boldsymbol{e} \in \mathscr{F}_h, \tag{2.4}$$

where $\mathscr{F}_h$ is the set of edges of $\mathscr{T}_h$. However, for the given metric $\mathcal{M}$, there does not exist (except special cases) any triangulation satisfying (2.4). Therefore, we define the triangulation *generated by metric* $\mathcal{M}$ such that (2.4) is satisfied approximately by the *least square technique*, see [9, 14].

Definition 2.3. *Let* $\mathcal{M} : \Omega \to \mathrm{Sym}$ *be the Riemann metric on* Ω*. We say that the triangulation* $\mathscr{T}_h$ *is* generated by metric $\mathcal{M}$ *if*

$$\mathscr{T}_h = \arg\min_{\mathscr{T}_h'} \sum_{\boldsymbol{e} \in \mathscr{F}_h'} \Big(\|\boldsymbol{e}\|_{\mathcal{M}} - \sqrt{3}\Big)^2, \tag{2.5}$$

where the minimum is taken over all possible triangulations $\mathscr{T}_h'$ *of* Ω *and* $\mathscr{F}_h'$ *is the set of edges of* $\mathscr{T}_h'$.

Let us note that there exist algorithms and codes, e.g., [10], [19], which construct mesh $\mathscr{T}_h$ for the given metric $\mathcal{M}$ in the sense of Definition 2.3. These algorithms are based on the combination of several local operations which minimize the right-hand side of (2.5). However, a different ordering of these operations lead to different (but similar) *hp*-grids. The mesh generation is fast in comparison to the numerical solution of the corresponding boundary value problem.

2.3 *hp*-mesh

Let $\mathscr{T}_h = \{K\}$ be a triangulation of Ω. To each $K \in \mathscr{T}_h$, we assign a positive integer p_K (=local polynomial approximation degree on K). Then we define the *polynomial degree set* $\mathsf{p} := \{p_K;\ K \in \mathscr{T}_h\}$. The pair $\mathscr{T}_{h\mathsf{p}} := \{\mathscr{T}_h, \mathsf{p}\}$ is called the *hp-mesh*. The polynomial degree set p can be defined in the following way.

Definition 2.4. *Let* $\mathcal{P} : \Omega \to \mathbb{R}^+$ *be the given integrable function, which we call the* polynomial degree distribution function*. Let* $\mathscr{T}_h$ *be a triangulation of* Ω*. Using* $\mathcal{P}$*, we define the polynomial degree set* $\mathsf{p} = \{p_K;\ K \in \mathscr{T}_h\}$ *by*

$$p_K := \mathrm{int}\left[\frac{1}{|K|}\int_K \mathcal{P}(x)\,\mathrm{d}x\right], \quad K \in \mathscr{T}_h, \tag{2.6}$$

where $\mathrm{int}[\cdot]$ *denotes the rounding to the nearest integer.*

Therefore, for the given Riemann metric $\mathcal{M} : \Omega \to \mathrm{Sym}$ and for the given polynomial degree distribution function $\mathcal{P} : \Omega \to \mathbb{R}^+$, we are able to construct the *hp*-mesh $\mathscr{T}_{h\mathsf{p}} = \{\mathscr{T}_h, \mathsf{p}\}$ where $\mathscr{T}_h$ and p are given by Definitions 2.3 and 2.4, respectively. Let us note that in practice, it is sufficient to evaluate $\mathcal{M}$ and $\mathcal{P}$ only in a finite number of nodes $x \in \Omega$.

3 Optimal anisotropic hp-mesh for the given function $u : \Omega \to \mathbb{R}$

This section exhibits a theoretical background of this paper. We employ several results from [13]. We formulate and (partly) solve the main problem, which defines the optimal anisotropic hp-mesh for the given function $u : \Omega \to \mathbb{R}$. The optimality is based on the minimization of number of degrees of freedom provided that the interpolation error in the broken H^1-seminorm is below the given tolerance. For simplicity, we deal with functions from $V := C^\infty(\Omega)$.

3.1 The main problem

For the given hp-mesh $\mathscr{T}_{h\mathsf{p}} = \{\mathscr{T}_h, \mathsf{p}\}$, we define the space of discontinuous piecewise polynomial functions by

$$S_{h\mathsf{p}} := \{v \in L^2(\Omega);\ v|_K \in P^{p_K}(K)\ \forall K \in \mathscr{T}_h\}, \tag{3.1}$$

where $P^{p_K}(K)$ is the space of polynomials of degree $\leq p_K$ on $K \in \mathscr{T}_h$. The dimension of $S_{h\mathsf{p}}$ is equal to $N_{h\mathsf{p}} := \sum_{K\in\mathscr{T}_h}(p_K+1)(p_K+2)/2$, which is called the *number of degrees of freedom* of the hp-mesh $\mathscr{T}_{h\mathsf{p}}$.

First, we introduce a local projection operator.

Definition 3.1. *Let $u \in V$ be the given function, $\bar{x} \in \Omega$ and $p \in \mathbb{N}$ be an integer. We define the mapping $\pi_{\bar{x},p} : V \to P^p(\bar{\Omega})$ such that*

$$\frac{\partial^k\, \pi_{\bar{x},p}u(\bar{x})}{\partial x_1^l \partial x_2^{k-l}} = \frac{\partial^k\, u(\bar{x})}{\partial x_1^l \partial x_2^{k-l}} \quad \forall l = 0,\dots,k \quad \forall k = 0,\dots,p. \tag{3.2}$$

Thus, $\pi_{\bar{x},p}u$ is the Taylor polynomial of degree p about $\bar{x} \in \Omega$. The existence and uniqueness of $\pi_{\bar{x},p}u$ is obvious. Using the mapping $\pi_{\bar{x},p}$, we define the projection into the space $S_{h\mathsf{p}}$.

Definition 3.2. *Let $\mathscr{T}_{h\mathsf{p}} = (\mathscr{T}_h, \mathsf{p})$ be a hp-mesh, x_K be the barycenter of $K \in \mathscr{T}_h$ and $S_{h\mathsf{p}}$ be the corresponding space of discontinuous piecewise polynomial functions given by* (3.1)*. We define the operator $\Pi_{h\mathsf{p}} : V \to S_{h\mathsf{p}}$ by*

$$(\Pi_{h\mathsf{p}}u)|_K := \pi_{x_K,p_K}(u|_K) \quad \forall K \in \mathscr{T}_h, \tag{3.3}$$

where π_{x_K,p_K} is given by (3.2). The operator $\Pi_{h\mathsf{p}}$is defined separately for each $K \in \mathscr{T}_h$ and it is unique for the given hp-mesh. In the analysis, we are interested in the optimization of the interpolation error $u - \Pi_{h\mathsf{p}}u$ in the *broken H^1-seminorm* defined by

$$|v|_{H^1(\mathscr{T}_h)} := \left(\sum_{K\in\mathscr{T}_h} |v|^2_{L^2(K)}\right)^{1/2}, \quad v \in \{w \in L^2(\Omega);\ w|_K \in H^1(K)\ \forall K \in \mathscr{T}_h\}.$$

Now, we are ready to formulate the following problem.

Problem 3.1. *Let $u \in V$ be the given function and $\omega > 0$ be the given tolerance. We* seek a hp-mesh $\mathscr{T}_{h\mathsf{p}}$ *(and therefore the corresponding space $S_{h\mathsf{p}}$) such that*

(P1) $|u - \Pi_{h\mathsf{p}}u|_{H^1(\mathscr{T}_h)} \leq \omega$, *where $\Pi_{h\mathsf{p}} : V \to S_{h\mathsf{p}}$ is defined by* (3.3)*,*

(P2) the number of degrees of freedom $N_{h\mathsf{p}}$ of $\mathscr{T}_{h\mathsf{p}}$ ($= \dim S_{h\mathsf{p}}$) is minimal.

The Problem 3.1 is complex and we are not able to solve it efficiently. Therefore, we introduce an *auxiliary* local *problem* whose solution is an optimal anisotropic element with the barycentre at the given node $\bar{x} \in \Omega$. Then, using the solution of the auxiliary problem and heuristic considerations, we derive the Riemann metric $\mathcal{M} : \Omega \to \mathrm{Sym}$ and the polynomial degree distribution function $\mathcal{P} : \Omega \to \mathbb{R}^+$, which define the hp-mesh $\mathscr{T}_{h\mathsf{p}}$. This hp-mesh satisfies condition (P1) of Problem 3.1 and the corresponding number $N_{h\mathsf{p}}$ is as small as we are able to achieve. Therefore, we expect that this resulting hp-mesh is close to the solution of Problem 3.1.

3.2 Auxiliary problem

Let $u \in V$, $\bar{x} = (\bar{x}_1, \bar{x}_2) \in \Omega$ and $p \in \mathbb{N}$ be given. Using the Taylor expansion of degree $p+1$ at $\bar{x}$, we have

$$u(x) = \sum_{k=0}^{p+1} \frac{1}{k!} \left(\sum_{l=0}^{k} \binom{k}{l} \frac{\partial^k u(\bar{x})}{\partial x_1^l \partial x_2^{k-l}} (x_1 - \bar{x}_1)^l (x_2 - \bar{x}_2)^{k-l} \right) + O(\theta^{p+2}), \ x \in \Omega, \tag{3.4}$$

where $\binom{k}{l} = \frac{k!}{l!(k-l)!}$ and $\theta = |x - \bar{x}|$. Let $\pi_{\bar{x},p} u$ be given by (3.2), then (3.4) reads

$$u(x) - \pi_{\bar{x},p} u(x) = e^{\mathrm{int}}_{\bar{x},p}(x) + O(\theta^{p+2}), \tag{3.5}$$

where

$$e^{\mathrm{int}}_{\bar{x},p}(x) := \frac{1}{(p+1)!} \sum_{l=0}^{p+1} \left[\binom{p+1}{l} \frac{\partial^{p+1} u(\bar{x})}{\partial x_1^l \partial x_2^{p+1-l}} (x_1 - \bar{x}_1)^l (x_2 - \bar{x}_2)^{p+1-l} \right] \tag{3.6}$$

is the *interpolation error function* of degree p located at $\bar{x}$. Obviously, $e^{\mathrm{int}}_{\bar{x},p}(\bar{x}) = 0$ and $e^{\mathrm{int}}_{\bar{x},p}(x) \approx u(x) - \pi_{\bar{x},p} u(x)$ up to the higher order terms. Moreover, (3.3) and (3.5) give

$$(u - \Pi_{h\mathsf{p}} u)\,|_K \approx e^{\mathrm{int}}_{x_K, p_K}|_K \quad \forall K \in \mathscr{T}_h, \tag{3.7}$$

where x_K is the barycentre of $K \in \mathscr{T}_h$.

Now, we introduce the following auxiliary local problem.

Problem 3.2. *Let $u \in V$, $\bar{x} \in \Omega$, $p \in \mathbb{N}$, and $\bar{\omega} > 0$ be given. We seek an* anisotropic triangle K *(i.e., its anisotropy $\{h_K, \sigma_K, \phi_K\}$, cf. Definition 2.2) having the barycentre at $\bar{x}$ such that*

(p1) $\left| e^{\mathrm{int}}_{\bar{x},p} \right|_{H^1(K)} \le \bar{\omega}$,

(p2) the area of K is the maximal possible.

The condition (p2) follows from the consideration that in order to minimize the number $N_{h\mathsf{p}}$ of the *hp*-mesh, we have to construct triangles with the maximal possible area (for the given polynomial approximation degree p).

3.3 Solution of the auxiliary problem

We write the function $e^{\mathrm{int}}_{\bar{x},p}$ defined by (3.6) in the form

$$e^{\mathrm{int}}_{\bar{x},p}(\xi) := \sum_{l=0}^{p+1} \alpha_l \xi_1^l \xi_2^{p+1-l}, \tag{3.8}$$

where $\xi_i := x_i - \bar{x}_i, \ i = 1, 2$, and

$$\alpha_l := \frac{1}{(p+1)!} \binom{p+1}{l} \frac{\partial^{p+1} u(\bar{x})}{\partial x_1^l \partial x_2^{p+1-l}}, \quad l = 0, \dots, p+1. \tag{3.9}$$

Using the definition of the H^1-seminorm, we have

$$\left| e^{\mathrm{int}}_{\bar{x},p} \right|^2_{H^1(K)} = \int_K |\nabla e^{\mathrm{int}}_{\bar{x},p}|^2 \, \mathrm{d}x. \tag{3.10}$$

Let us consider the integrand of (3.10). Taking into account (3.8)–(3.9), we have

$$\begin{aligned} |\nabla e^{\mathrm{int}}_{\bar{x},p}(x)|^2 &= \left(\frac{\partial}{\partial x_1} \sum_{l=0}^{p+1} \alpha_l \xi_1^l \xi_2^{p+1-l} \right)^2 + \left(\frac{\partial}{\partial x_2} \sum_{l=0}^{p+1} \alpha_l \xi_1^l \xi_2^{p+1-l} \right)^2 \\ &= \left(\sum_{l=1}^{p+1} l\, \alpha_l \xi_1^{l-1} \xi_2^{p+1-l} \right)^2 + \left(\sum_{l=0}^{p} (p+1-l) \alpha_l \xi_1^l \xi_2^{p-l} \right)^2 \\ &= \left(\sum_{l=0}^{p} \beta_l^{(1)} \xi_1^l \xi_2^{p-l} \right)^2 + \left(\sum_{l=0}^{p} \beta_l^{(2)} \xi_1^l \xi_2^{p-l} \right)^2, \end{aligned} \tag{3.11}$$

where

$$\beta_l^{(1)} := (l+1)\, \alpha_{l+1}, \quad \beta_l^{(2)} := (p+1-l)\, \alpha_l, \quad l = 0, \dots, p. \tag{3.12}$$

In order to simplify the last terms in (3.11), we introduce the following Lemma.

Lemma 3.1. *Let $\beta_l \in \mathbb{R}$ for $l = 0, \dots, p$. Then*

$$\left(\sum_{l=0}^{p} \beta_l \xi_1^l \xi_2^{p-l} \right)^2 = \sum_{i=0}^{2p} \gamma_i \xi_1^i \xi_2^{2p-i}, \tag{3.13}$$

where

$$\gamma_i = \sum_{j=1}^{i} \beta_j \beta_{i-j}, \qquad \gamma_{2p-i} = \sum_{j=0}^{i} \beta_{p-j} \beta_{p-(i-j)}, \qquad i = 0, \dots, p.$$

Proof. The identity can be derived by a direct computation. □

A direct consequence of (3.8), (3.11) and Lemma 3.1 is the following:

Lemma 3.2. *Let $e^{\mathrm{int}}_{\bar{x},p}$ be the interpolation error function* (3.6) *written in the form* (3.8)–(3.9). *Then*

$$|\nabla e^{\mathrm{int}}_{\bar{x},p}(x)|^2 = \sum_{i=0}^{2p} \gamma_i (x_1 - \bar{x}_1)^i (x_2 - \bar{x}_2)^{2p-i}, \tag{3.14}$$

where $\gamma_i = \sum_{j=1}^{i} (\beta_j^{(1)} \beta_{i-j}^{(1)} + \beta_j^{(2)} \beta_{i-j}^{(2)})$, $\gamma_{2k-i} = \sum_{j=1}^{i} (\beta_{p-j}^{(1)} \beta_{p-(i-j)}^{(1)} + \beta_{p-j}^{(2)} \beta_{p-(i-j)}^{(2)})$, $i = 0, \dots, p$, and $\beta_l^{(1)}$, $\beta_l^{(2)}$, $l = 0, \dots, p$ are given by (3.12).

Lemma 3.2 implies that $|\nabla e^{\mathrm{int}}_{\bar{x},p}|^2$ is a polynomial function of degree $2p$, i.e., a function depending on $2p + 1$ coefficients. On the other hand, the sought anisotropy of a triangle is given by three parameters. Therefore, in order to solve Problem 3.2, it is advantageous to bound $|\nabla e^{\mathrm{int}}_{\bar{x},p}|^2$ by an expression depending on three parameters. Motivated by [4, 5], we derived in [13] the bound of the *interpolation error function* (which is the polynomial function of degree $p + 1$) in the form

$$\left| e^{\mathrm{int}}_{\bar{x},p}(x) \right| \le \bar{A}_p \left((x - \bar{x})^{\mathrm{T}} \mathbb{Q}_{\bar{\varphi}_p} \bar{\mathbb{D}}_{\rho_p} \mathbb{Q}^{\mathrm{T}}_{\bar{\varphi}_p} (x - \bar{x}) \right)^{\frac{p+1}{2}} \ \forall\, x \in \Omega, \tag{3.15}$$

where $\bar{A}_p > 0$, $\mathbb{Q}_{\bar{\varphi}_p}$ is the rotation matrix about the angle $\bar{\varphi}_p$ and $\bar{\mathbb{D}}_{\rho_p}$ is the matrix given by

$$\bar{\mathbb{D}}_{\rho} := \begin{pmatrix} 1 & 0 \\ 0 & \rho^{-\frac{2}{p+1}} \end{pmatrix}, \quad \rho \ge 1. \tag{3.16}$$

By virtue of (3.15)–(3.16), we seek a *bound of the magnitude of the gradient of the interpolation error functions* (which is the polynomial of degree $2p$) in the form

$$\left| \nabla e^{\mathrm{int}}_{\bar{x},p}(x) \right|^2 \le A_p \left((x - \bar{x})^{\mathrm{T}} \mathbb{Q}_{\varphi_p} \mathbb{D}_{\rho_p} \mathbb{Q}^{\mathrm{T}}_{\varphi_p} (x - \bar{x}) \right)^{p} \ \forall\, x \in \Omega, \tag{3.17}$$

where $A_p > 0$, $\mathbb{Q}_{\varphi_p}$ is the rotation about the angle φ_p and $\mathbb{D}_{\rho_p}$ is given by

$$\mathbb{D}_{\rho} := \begin{pmatrix} 1 & 0 \\ 0 & \rho^{-1/p} \end{pmatrix}, \quad \rho \ge 1. \tag{3.18}$$

The values $A_p \ge 0$, $\rho_p \ge 1$ and $\varphi_p \in [0, 2\pi)$ represent the *size*, the *aspect ratio* and the *orientation* of the square of the magnitude of the gradient of the interpolation error functions $|\nabla e^{\mathrm{int}}_{\bar{x},p}|^2$ and they are defined in such a way that the bound (3.17) is as sharp as possible in the following sense:

Obviously, both sides of (3.17) are $2p$-homogeneous functions of $(x - \bar{x})$, i.e., $f(x - \bar{x}) = |x - \bar{x}|^{2p} f(\frac{x - \bar{x}}{|x - \bar{x}|})$. Hence, it is enough to verify (3.18) for $x \in \Omega$, $|x - \bar{x}| = 1$. Moreover, both sides of (3.17) define bounded domains F^p and G^p in $\mathbb{R}^2$, namely F^p and G^p are the interiors of the closed curves

$$\begin{aligned} &\left\{ y \in \mathbb{R}^2;\ y = \left| \nabla e^{\mathrm{int}}_{\bar{x},p}(x) \right|^2 (x - \bar{x}),\ |x - \bar{x}| = 1 \right\} \text{ and} \\ &\left\{ y \in \mathbb{R}^2;\ y = A_p \left((x - \bar{x})^{\mathrm{T}} \mathbb{Q}_{\varphi_p} \mathbb{D}_{\rho_p} \mathbb{Q}^{\mathrm{T}}_{\varphi_p} (x - \bar{x}) \right)^{p} (x - \bar{x}),\ |x - \bar{x}| = 1 \right\}, \end{aligned} \tag{3.19}$$

respectively.

Obviously, if $F^p \subset G^p$ then (3.17) is valid. Therefore, in order to guarantee sharpness of (3.17), we set parameters $A_p \ge 0$, $\rho_p \ge 1$ and $\varphi_p \in [0, 2\pi)$ in such a way that $F^p \subset G^p$ and the area of G^p is minimal.

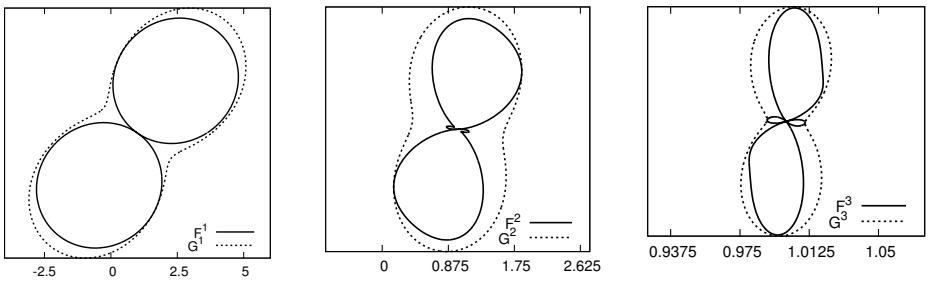

Fig. 2: Boundaries of F^p, G^p, $p = 1, 2, 3$ for Example 3.1.

Definition 3.3. *The triplet* $\{A_p,\ \rho_p,\ \varphi_p\}$ *arising in* (3.17) *is called the* anisotropy *of the magnitude of the gradient of the interpolation error function* $|\nabla e^{\mathrm{int}}_{\bar{x},p}|^2$.

Remark 3.1. *The triplet* $\{A_p,\ \rho_p,\ \varphi_p\}$ *can be easily found numerically with the aid of the algorithm introduced in [13, Section 3.2]. First, we set the triplet* $\{\tilde{A}_p,\ \tilde{\rho}_p,\ \tilde{\varphi}_p\}$, *where* $\tilde{A}_p$ *is the maximal value of* $|\nabla e^{\mathrm{int}}_{\bar{x},p}(\bar{x}+\xi)|$ *for* $\xi \in \mathbb{R}^2,\ |\xi| = 1$ *given by* (3.14), $\tilde{\varphi}_p$ *is the angle of the direction* ξ *along which the maximal value* $|\nabla e^{\mathrm{int}}_{\bar{x},p}(\bar{x}+\xi)|$ *is attained and* $\tilde{\rho}_p$ *is the ratio between* $\tilde{A}_p$ *and the value of* $|\nabla e^{\mathrm{int}}_{\bar{x},p}(\bar{x}+\xi)|$ *along the direction perpendicular to the direction with the maximal value.*

However, in the general case, inequality (3.17) *is not valid for* $\{\tilde{A}_p, \tilde{\rho}_p, \tilde{\varphi}_p\}$. *Therefore, the triplet* $\{\tilde{A}_p, \tilde{\rho}_p, \tilde{\varphi}_p\}$ *has to be modified in such a way that the corresponding set* G^p *is increased in order to contain* F^p.

Example 3.1. *Figure 2 shows the sets* F^p *and* G^p *for* $p = 1, 2, 3$, $\bar{x} = (1, 1)$ *and*

$$u(x_1, x_2) = 0.01(6x_1^7 + 4x_1^6x_2 - 3x_1^5x_2^2 + 8x_1^4x_2^3 + 12x_1^3x_2^4 + 5x_1^2x_2^5 + x_1x_2^6 - x_2^7).$$

The bound (3.17) is the basis for the solution of Problem 3.2 formulated below.

Theorem 3.1. *Let* $u \in V$, $\bar{x} \in \Omega$, $p \in \mathbb{N}$, *and* $\bar{\omega} > 0$ *be given. Let* $\{A_p, \varphi_p, \rho_p\}$ *be the anisotropy of the gradient of the corresponding interpolation error function* $e^{\mathrm{int}}_{\bar{x},p}$ *satisfying* (3.17). *We set* $\nu_{\bar{x},p}$ *by*

$$\nu_{\bar{x},p} := \left(\bar{\omega}^2 \rho_p^{\frac{1}{2}}/(c_p A_p)\right)^{1/(p+1)}, \tag{3.20}$$

where $c_p := \frac{\pi^{-p}}{p+1}$ *and* $\pi = 3.1415\ldots$. *Then the triangle* $K_{\bar{x},p}$ *with the anisotropy* $\{h_E, \sigma_E, \phi_E\}$ *given by*

$$h_E = \left(\rho_p^{\frac{1}{2p}}\, \nu_{\bar{x},p}/\pi\right)^{1/2}, \quad \sigma_E = \rho_p^{\frac{1}{2p}}, \quad \phi_E = \varphi_p - \pi/2 \tag{3.21}$$

is (almost) the solution of Problem 3.2, namely we have

$$\left|e^{\mathrm{int}}_{\bar{x},p}\right|_{H^1(K_{\bar{x},p})} \le \left(c_p A_p \rho_p^{-\frac{1}{2}}\, (\nu_{\bar{x},p})^{p+1}\right)^{1/2} = \bar{\omega}. \tag{3.22}$$

The word "almost" means that the condition (p1) in Problem 3.2 is satisfied and the condition (p2) is satisfied up to a replacement of K *by its corresponding ellipse, cf. Definition 2.1.*

Proof. The proof uses the same technique as the derivation of [13, Lemma 3.15]. Since it is relatively long, we present only the main steps.

(i) Instead of maximization of the area K for fixed error $\left|e^{\mathrm{int}}_{\bar{x},p}\right|_{H^1(K)} = \bar{\omega}$, we fix the area K and minimize the error $\left|e^{\mathrm{int}}_{\bar{x},p}\right|_{H^1(K)}$. These tasks are equivalent.

(ii) In order to simplify the integration, we replace triangle $K_{\bar{x},p}$ by the corresponding ellipse $E_{\bar{x},p}$, cf. Definition 2.1. Obviously, $\left|e^{\mathrm{int}}_{\bar{x},p}\right|_{H^1(K_{\bar{x},p})} \le \left|e^{\mathrm{int}}_{\bar{x},p}\right|_{H^1(E_{\bar{x},p})}$.

(iii) We denote by h_E and $h_E^\perp = h_E/\sigma_E$ the size of the semi-axes of the sought ellipse $E_{\bar{x},p}$ and the angle between the main axes of E and axis x_1 by ϕ_E. Let $\hat{E} := \{\xi \in \mathbb{R}^2;\, |\xi| \le 1\}$ be the closed unit ball (= the reference circle), we define the mapping $\boldsymbol{F}_E : \hat{E} \to \mathbb{R}^2$ by $\boldsymbol{F}_E(\hat{x}) := \mathbb{Q}_{\phi_E}\mathbb{S}_E\hat{x} + \bar{x}$, where $\mathbb{Q}_{\phi_E}$ is the rotation about the angle ϕ_E and $\mathbb{S}_E = \operatorname{diag}\left(h_E, h_E^\perp\right) = h_E \operatorname{diag}\left(1, \sigma_E^{-1}\right)$. We can simply verify that $\boldsymbol{F}_E$ maps $\hat{E}$ onto $E_{\bar{x},p}$, i.e., $\boldsymbol{F}_E(\hat{E}) = E_{\bar{x},p}$.

(iv) Furthermore, the definition of the mapping $\boldsymbol{F}_E$ gives the implications

$$x = \boldsymbol{F}_E(\hat{x}) \quad \Rightarrow \quad x - \bar{x} = \mathbb{Q}_{\phi_E}\mathbb{S}_E\hat{x} \quad \Rightarrow \quad (x-\bar{x})^{\mathrm{T}} = \hat{x}^{\mathrm{T}}\mathbb{S}_E^{\mathrm{T}}\mathbb{Q}_{\phi_E}^{\mathrm{T}}. \tag{3.23}$$

The Jacobi matrix $\frac{D\boldsymbol{F}_E}{D\hat{x}}$ has the determinant equal to $h_E h_E^\perp$ and the area of the ellipse $E_{\bar{x},p}$ is equal to

$$\nu_{\bar{x},p} := \pi h_E h_E^\perp = \pi h_E^2/\sigma_E. \tag{3.24}$$

(v) With the aid of (3.17), the theorem of substitution and (3.23), we have

$$\begin{aligned}\left|e^{\mathrm{int}}_{\bar{x},p}\right|^2_{H^1(E_{\bar{x},p})} &= \int_{E_{\bar{x},p}} \left|\nabla e^{\mathrm{int}}_{\bar{x},p}(x)\right|^2 \mathrm{d}x \le \int_{E_{\bar{x},p}} A_p \left((x-\bar{x})^{\mathrm{T}}\mathbb{Q}_{\varphi_p}\mathbb{D}_{\rho_p}\mathbb{Q}_{\varphi_p}^{\mathrm{T}}(x-\bar{x})\right)^p \mathrm{d}x \\ &= \int_{\hat{E}} A_p \left(\hat{x}^{\mathrm{T}}\mathbb{S}_E^{\mathrm{T}}\mathbb{Q}_{\phi_E}^{\mathrm{T}}\mathbb{Q}_{\varphi_p}\mathbb{D}_{\rho_p}\mathbb{Q}_{\varphi_p}^{\mathrm{T}}\mathbb{Q}_{\phi_E}\mathbb{S}_E\hat{x}\right)^p h_E h_E^\perp \,\mathrm{d}\hat{x}.\end{aligned}$$

(vi) After some manipulations, we derive the inequality

$$\left|e^{\mathrm{int}}_{\bar{x},p}\right|^2_{H^1(E_{\bar{x},p})} \le A_p \left(\frac{\nu_{\bar{x},p}}{\pi}\right)^{p+1} \int_{\hat{E}} \left(\hat{x}^{\mathrm{T}}\bar{\mathbb{G}}\hat{x}\right)^p \mathrm{d}\hat{x}, \tag{3.25}$$

where

$$\bar{\mathbb{G}} := \begin{pmatrix} \sigma_E(\cos^2\tau + \rho_p^{-\frac{1}{p}}\sin^2\tau) & -\sin\tau\cos\tau(1-\rho_p^{-\frac{1}{p}}) \\ -\sin\tau\cos\tau(1-\rho_p^{-\frac{1}{p}}) & \sigma_E^{-1}(\sin^2\tau + \rho_p^{-\frac{1}{p}}\cos^2\tau) \end{pmatrix}, \quad \tau := \phi_E - \varphi_p.$$

(vii) We find that right-hand side of (3.25) is minimal if matrix $\bar{\mathbb{G}}$ is diagonal and both diagonal terms are equal. Hence, taking into account that $\sigma_E \ge 1$ and $\rho_p \ge 1$, we obtain $\cos\tau = 0$ and consequently

$$\tau = \phi_E - \varphi_p = \pi/2 \quad \& \quad \sigma_E = \rho_p^{\frac{1}{2p}}. \tag{3.26}$$

(viii) Finally, inserting (3.26) in (3.25), we have

$$\left|e^{\mathrm{int}}_{\bar{x},p}\right|^2_{H^1(E_{\bar{x},p})} \le A_p\left(\frac{\nu_{\bar{x},p}}{\pi}\right)^{p+1} \int_{\hat{E}} \left(\rho_p^{-\frac{1}{2p}}|\hat{x}|^2\right)^p \mathrm{d}\hat{x} = A_p \left(\frac{\nu_{\bar{x},p}}{\pi}\right)^{p+1} \rho_p^{-\frac{1}{2}} \frac{2\pi}{2p+2},$$

which together with (3.24) and (3.26) proves the theorem.

□

Finally, let us note that the value $\nu_{\bar{x},p}$ is equal to the area of element (up to a multiplicative constant) and due to (3.20), it is related to the local tolerance $\bar{\omega}$. It will be specified in the following section.

3.4 Setting of the size of a triangle

We need to set the area $\nu_{\bar{x},p}$ of a triangle, i.e., its size since its ratio was already specified. The main Problem 3.1 requires the error bound $|u - \Pi_{hp}u|_{H^1(\mathscr{T}_h)} \le \omega$, where $\omega > 0$ is the given (global) tolerance. In order to set $\bar{\omega}$ in Problem 3.2, we use the implication

$$|u - \Pi_{hp}u|_{H^1(\mathscr{T}_h)} \le \omega \quad \Longleftarrow \quad |u - \Pi_{hp}u|_{H^1(K)} \le \omega\,(|K|/|\Omega|)^{1/2} \;\; \forall K \in \mathscr{T}_h. \tag{3.27}$$

Although the *equidistribution condition* on the right-hand side of (3.27) *does not guarantee* that the resulting grid is the globally optimal grid, we employ it for the setting of the local tolerance $\bar{\omega}$ in (3.20), since we do know how to solve this complex problem in an effective way.

In virtue of (3.7) and the right-hand side of (3.27), we require that

$$\left|e^{\mathrm{int}}_{\bar{x},p}\right|_{H^1(K_{\bar{x},p})} \le \omega\,(\nu_{\bar{x},p}/|\Omega|)^{1/2}. \tag{3.28}$$

Hence, in order to specify the area $\nu_{\bar{x},p}$, using (3.22) and (3.28), we set the condition $c_p A_p \rho_p^{-\frac{1}{2}} (\nu_{\bar{x},p})^{p+1} = \omega^2 \nu_{\bar{x},p}/|\Omega|$, which implies

$$\nu_{\bar{x},p} = \left(\frac{\omega^2 \rho_p^{\frac{1}{2}}}{|\Omega| c_p A_p} \right)^{1/p}. \tag{3.29}$$

3.5 Choice of the polynomial approximation degree

In previous sections, we have derived the anisotropy of the optimal triangle $K_{\bar{x},p}$, which minimizes the norm of the interpolation error function $e^{\text{int}}_{\bar{x},p}$ on $K_{\bar{x},p}$ for any $\bar{x} \in \Omega$ and for an arbitrary given polynomial approximation degree p. In this section, we set the optimal polynomial degree p.

We introduced the so-called *density of the number of degrees of freedom* (DOF) by

$$\eta_p(\bar{x}) := \frac{(p+1)(p+2)}{2\nu_{\bar{x},p}}, \quad p \in \mathbb{N},\ \bar{x} \in \Omega \tag{3.30}$$

representing the number of degree of freedom per unit area. A formal integration of (3.30) over Ω gives the total number of DOF. Hence, in order to minimize the number of DOF, we minimize the integrand $\eta_p(\bar{x})$. Therefore, for each $\bar{x} \in \Omega$, we choose the polynomial degree $p \in \mathbb{N}$ such that the corresponding value $\eta_{\bar{x},p}$ is minimal, i.e., we put

$$p_{\bar{x}} := \arg\min_{p \in \mathbb{N}} \eta_p(\bar{x}). \tag{3.31}$$

Let us note that in practical implementation, the degree p is bounded from above by $p_{\max}$ (= the maximal implemented polynomial approximation degree), hence the minimum in (3.31) always exists.

3.6 Anisotropic hp-adaptation algorithm

Now we are ready to define the Riemann metric $\mathcal{M}$ and the polynomial degree distribution function $\mathcal{P}$, which generate the hp-mesh $\mathscr{T}_{h\mathsf{p}}$ by Definitions 2.3 and 2.4, such that $\mathscr{T}_{h\mathsf{p}}$ is "close" to the solution of the main Problem 3.1. The word "close" means the best hp-mesh which we are able to achieve. It is possible to show that for some special problems, the resulting hp-grid is exactly the solution of Problem 3.1. We introduce the following algorithm.

Algorithm 1 Generation of $\mathcal{M}(x)$ and $\mathcal{P}(x)$ for $x \in \Omega$

let $u \in V$ and $\omega > 0$ be given
for all $p = 1, 2, \ldots, p_{\max}$ **do**
  evaluate the anisotropy $\{A_p, \varphi_p, \rho_p\}$ introduced in Definition 3.3
  using (3.29), set the area $\nu_p(x)$ of the triangle $K_{x,p}$
  using (3.21), set the anisotropy of triangle $K_{x,p}$ by $\{h_E(x), \sigma_E(x), \phi_E(x)\}$
  using Definition 2.2, set matrix $\mathbb{M}_p(x)$ defining $K_{x,p}$
  using (3.30), evaluate the quantity $\eta_p(x) := (p+1)(p+2)/(2\nu_p(x))$
end for
find $p_x \in \mathbb{N}$ minimizing $\eta_p(x)$, i.e. $p_x := \arg\min_{p=1,\ldots,p_{\max}} \eta_p(x)$.
set $\mathcal{M}(x) := \mathbb{M}_{p_x}(x)$ and $\mathcal{P}(x) := p_x$.

Theoretically, we can employ the previous algorithm for any $x \in \Omega$. In practical applications, we evaluate $\mathcal{M}$ and $\mathcal{P}$ only for a finite number of $x \in \Omega$ and then we continuously interpolate $\mathcal{M}$ and $\mathcal{P}$ on Ω.

3.7 Extension to $W^{k,q}$-seminorm

The previous technique can be extended to the mesh optimization with respect to the broken $W^{k,q}$-seminorm for $k \geq 1$ and $q \in [1, \infty]$. First, let us discuss the case $k = 1$ and $q < \infty$. Using (3.17), the

corresponding modification of step (v) in the proof of Theorem 3.1 leads to

$$\left|e^{\mathrm{int}}_{\bar{x},p}\right|^q_{W^{1,q}(E_{\bar{x},p})} = \int_{E_{\bar{x},p}} \left|\nabla e^{\mathrm{int}}_{\bar{x},p}(x)\right|^q \,\mathrm{d}x = \int_{E_{\bar{x},p}} \left(\left|\nabla e^{\mathrm{int}}_{\bar{x},p}(x)\right|^2\right)^{q/2} \mathrm{d}x$$
$$\leq \int_{E_{\bar{x},p}} \left(A_p \left((x-\bar{x})^{\mathrm{T}} \mathbb{Q}_{\varphi_p} \mathbb{D}_{\rho_p} \mathbb{Q}^{\mathrm{T}}_{\varphi_p} (x-\bar{x})\right)^p\right)^{q/2} \mathrm{d}x.$$

Then the consequent steps has to be modified appropriately.

Furthermore, for $k > 1$, its is necessary to evaluate the k^{th}-order derivative of the interpolation error function, namely $|\nabla^k e^{\mathrm{int}}_{\bar{x},p}(x)|^2$. After some calculation it would be possible to derive analogue to Lemma 3.2, whose result is a polynomial of degree $2(p+1-k)$. However, there is a restriction $k \leq p+1$. Otherwise, the corresponding seminorm vanishes. Finally, the case $q = \infty$ is simpler and can be carried out analogously.

4 Application of Algorithm 1 to the numerical solution of BVP

Algorithm 1 defines an anisotropic *hp*-mesh for the given function $u : \Omega \to \mathbb{R}$ which is optimal in the broken H^1-seminorm. This algorithm can be employed for the numerical solution of boundary value problems (BVP) where the function u represents the exact solution.

Since u is unknown, we replace it by the approximate solution $u_{h\mathsf{p}} \in S_{h\mathsf{p}}$ of BVP. Using a higher-order reconstruction, we approximate the anisotropy of the magnitude of the gradient of the interpolation error function. Then, using Algorithm 1, we generate a new (better) mesh $\mathscr{T}^N_{h\mathsf{p}}$ where the more accurate approximate solution can be obtained. The whole iteration loop is repeated until a desired stopping criterion is achieved. The mesh $\mathscr{T}^N_{h\mathsf{p}}$ is generated by our in-house code ANGENER [10], some implementation details can be found in [13].

5 Numerical examples

In this section, we present numerical examples, which demonstrate the efficiency of the proposed anisotropic *hp*-adaptive method in comparison with other adaptive techniques. We consider two linear convection-diffusion problems which are solved with the aid of the *discontinuous Galerkin method* (DGM). We employ the incomplete interior penalty Galerkin (IIPG) variant of DGM, which was analysed in several papers [7, 27, 11], the used solution strategy is given in [12].

5.1 Linear convection-diffusion equation with boundary layers

We consider the scalar linear convection-diffusion equation (similarly as in [6, 15])

$$-\varepsilon \triangle u - \frac{\partial u}{\partial x_1} - \frac{\partial u}{\partial x_2} = g \quad \text{in } \Omega = (0,1)^2, \tag{5.1}$$

where $\varepsilon > 0$ is a constant diffusion coefficient. We prescribe the Dirichlet boundary condition on $\partial\Omega$ and the source term g such that the exact solution has the form

$$u(x_1, x_2) = \left(c_1 + c_2(1-x_1) + e^{-x_1/\varepsilon}\right)\left(c_1 + c_2(1-x_2) + e^{-x_2/\varepsilon}\right) \tag{5.2}$$

with $c_1 = -e^{-1/\varepsilon}$ and $c_2 = -1 - c_1$. The solution contains two boundary layers along $x_1 = 0$ and $x_2 = 0$, whose width is proportional to ε. Here we consider $\varepsilon = 10^{-2}$ and $\varepsilon = 10^{-3}$. This example is suitable for the anisotropic adaptation since thin and long triangles can be employed in the boundary layers.

In order to demonstrate the efficiency of the presented method in comparison with other approaches, we carried out the following types of the mesh adaptation:

- isotropic *hp*-adaptive algorithm,
- anisotropic *h*-adaptive algorithm with the fixed $p = 3$,
- anisotropic *hp*-adaptive algorithm from [13], which optimizes the *hp*-mesh with respect to the L^2-norm,
- the presented anisotropic *hp*-adaptive Algorithm 1, which optimizes the *hp*-mesh with respect to the broken H^1-seminorm.

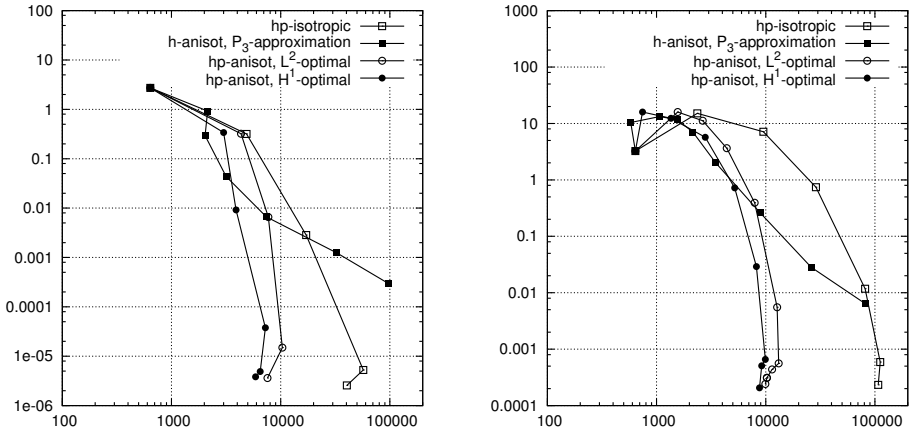

$\varepsilon = 10^{-2}$ $\varepsilon = 10^{-3}$

Fig. 3: Example (5.1), convergence of the errors in the broken H^1-seminorm with respect to DOF.

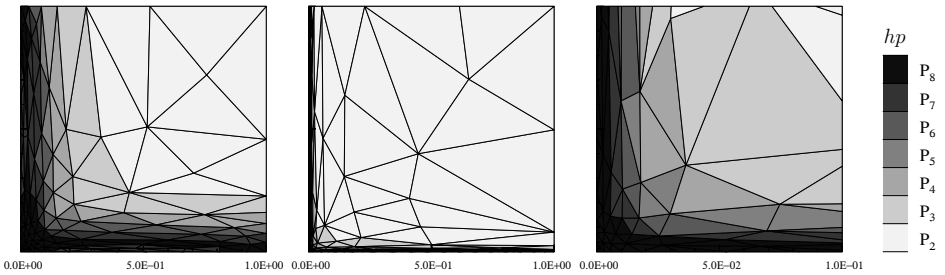

$\varepsilon = 10^{-2}$ $\varepsilon = 10^{-3}$ $\varepsilon = 10^{-3}$ (zoom)

Fig. 4: Example (5.1), the final *hp*-meshes.

We investigate the convergence of these algorithms in the broken H^1-seminorm with respect to the number of degrees of freedom, the results are plotted in Figure 3. We observe an evident efficiency of the anisotropic *hp*-method in comparison to the isotropic *hp*- as well as anisotropic *h*-methods. Moreover, the anisotropic *hp*-method based on the optimization with respect to the broken H^1-seminorm is a little more efficient than that one based on the optimization with respect to the L^2-norm which is in agreement with our expectations.

Furthermore, Algorithm 1 seems to be exponentially convergent, which means that the decrease of the error is faster than any linear decrease in logarithmic scale. We also observe that when Algorithm 1 is approaching to the prescribed error tolerance, it reduces the computational error as well as the number of degrees of freedom. The final *hp*-grids are showed in Figure 4, each element is drawn in the grey scale colour corresponding to the polynomial approximation degree.

5.2 Double curved interior layers problem

We consider a linear convection-dominated problem [18, Example 6.2]

$$-\varepsilon\triangle u + b_1\frac{\partial u}{\partial x_1} + b_2\frac{\partial u}{\partial x_2} = 0 \quad \text{in } \Omega = (0,1)^2, \tag{5.3}$$

where $\varepsilon = 10^{-6}$ and $(b_1, b_2) = (-x_2, x_1)$, is the velocity field with curved characteristics. We prescribe the homogeneous Neumann data at the outflow part $\partial\Omega_N = \{0\} \times (0,1)$ and the discontinuous Dirichlet data $u = 1$ at $(x_1, x_2) \in (\frac{1}{3}, \frac{2}{3}) \times \{0\}$ and $u = 0$ elsewhere on $\partial\Omega_D := \partial\Omega \setminus \partial\Omega_N$. Then this discontinuous profile is basically transported along the characteristic curves leading to sharp characteristic interior layers.

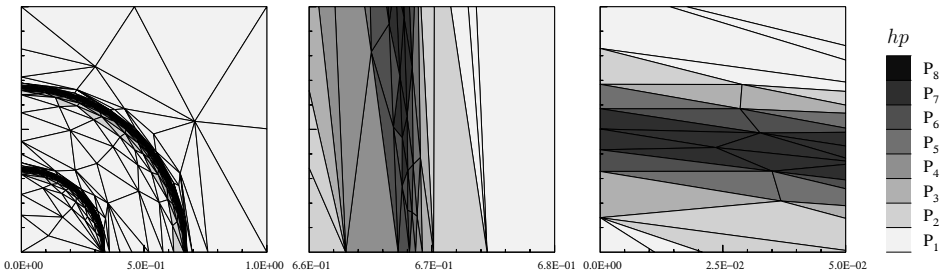

Fig. 5: Example (5.2), the final *hp*-mesh (left), 50x zoom of the begin of the outer arc (centre) and 20x zoom of the end of the inner arc (right).

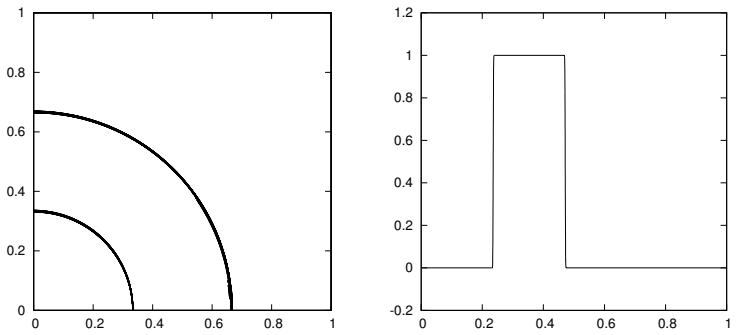

Fig. 6: Example (5.2), the isolines of the solution (left) and the diagonal cut (right).

We investigate the ability of the proposed anisotropic *hp*-algorithm to capture the sharp curved interior layers. Figure 5 shows the final *hp*-grid with the zooms of both interior layer. Furthermore, Figure 6 shows the isolines of the solution obtained on the final grid and the diagonal cut of the approximate solution along $x_2 = x_1$. We observe a sharp capturing of the both interior layers without any overshoots and undershoots of the solution. We recall that no stabilization technique (see, e.g., [17]) was used in the discontinuous Galerkin solver.

6 Conclusion

We presented the technique which generates anisotropic *hp*-grids based on the interpolation error estimates in the broken H^1-seminorm. These grids were employed for the numerical solution of second order boundary value problems with the aid of the discontinuous Galerkin method. Although the presented numerical examples demonstrate the efficiency of this approach in comparison to isotropic *hp*- as well as anisotropic *h*-methods we have no information about the computational error. We suppose that it will be possible to combine this approach with some a posteriori error estimation technique. Particularly, we expect that a posteriori error estimate gives us the information about the size of the error and the presented technique about the anisotropy of the elements. This is the subject of the future research.

References

[1] Ait-Ali-Yahia, D., Baruzzi, G., Habashi, W. G., Fortin, M., Dompierre, J., Vallet, M.-G.: Anisotropic mesh adaptation: towards user-independent, mesh-independent and solver-independent CFD. II. Structured grids. Internat. J. Numer. Methods Fluids **39** (2002), 657–673.

[2] Aubry, R. and Löhner, R.: Generation of viscous grids at ridges and corners. Int. J. Numer. Methods in Engng **77** (2009).

[3] Babuška, I. and Suri, M.: The *p*- and *hp* versions of the finite element method, basic principles and properties. SIAM Review **36** (1994), 578–632.

[4] Cao, W.: Anisotropic measures of third order derivatives and the quadratic interpolation error on triangular elements. SIAM J. Sci. Comput. **29** (2007), 756–781.

[5] Cao, W.: An interpolation error estimate in R^2 based on the anisotropic measures of higher order derivatives. Math. Comp. **77** (2008), 265–286.

[6] Clavero, C., Gracia, J.L., and Jorge, J.C.: A uniformly convergent alternating direction (HODIE) finite difference scheme for 2D time-dependent convection-diffusion problems. IMA J. Numer. Anal. **26** (2006), 155–172.

[7] Dawson, C.N., Sun, S., and Wheeler, M.F.: Compatible algorithms for coupled flow and transport. Comput. Methods Appl. Mech. Engng. **193** (2004), 2565–2580.

[8] Demkowicz, L., Rachowicz, W., and Devloo, P.: A fully automatic *hp*-adaptivity. J. Sci. Comput. **17** (2002), 117–142.

[9] Dolejší, V.: Anisotropic mesh adaptation for finite volume and finite element methods on triangular meshes. Comput. Vis. Sci. **1** (1998), 165–178.

[10] Dolejší, V.: *ANGENER – software package*. Charles University Prague, Faculty of Mathematics and Physics, 2000. www.karlin.mff.cuni.cz/ dolejsi/angen.html.

[11] Dolejší, V.: Analysis and application of IIPG method to quasilinear nonstationary convection-diffusion problems. J. Comp. Appl. Math. **222** (2008), 251–273.

[12] Dolejší, V.: *hp*-DGFEM for nonlinear convection-diffusion problems. Math. Comput. Simul. **87** (2013), 87–118.

[13] Dolejší, V.: Anisotropic *hp*-adaptive method based on interpolation error estimates in the L^q-norm. Appl. Numer. Math. **82** (2014), 80–114.

[14] Dolejší, V. and Felcman, J.: Anisotropic mesh adaptation and its application for scalar diffusion equations. Numer. Methods Partial Differential Equations **20** (2004), 576–608.

[15] Dolejší, V. and Roos, H.G.: BDF-FEM for parabolic singularly perturbed problems with exponential layers on layer-adapted meshes in space. Neural Parallel Sci. Comput. **18** (2010), 221–235.

[16] Frey, P.J. and Alauzet, F.: Anisotropic mesh adaptation for CFD computations. Comput. Methods Appl. Mech. Engrg. **194** (2005), 5068–5082.

[17] John, V. and Knobloch, P.: On spurious oscillations at layer diminishing (SOLD) methods for convection–diffusion equations: Part I – A review. Comput. Methods Appl. Mech. Engrg. **196** (2007), 2197–2215.

[18] Knopp, T., Lube, G., and Rapin, G.: Stabilized finite element methods with shock capturing for advection–diffusion problems. Comput. Methods Appl. Mech. Engrg. **191** (2002), 2997–3013.

[19] Laug, P. and Borouchaki, H.: *BL2D-V2: isotropic or anisotropic 2D mesher*. INRIA, 2002. https://www.rocq.inria.fr/gamma/Patrick.Laug/logiciels/ bl2d-v2/INDEX.html.

[20] Loseille, A. and Alauzet, F.: Continuous mesh framework part I: well-posed continuous interpolation error. SIAM J. Numer. Anal. **49** (2011), 38–60.

[21] Loseille, A. and Alauzet, F.: Continuous mesh framework part II: validations and applications. SIAM J. Numer. Anal. **49** (2011), 61–86.

[22] Mirebeau, J.M.: Optimal meshes for finite elements of arbitrary order. Constr. Approx. **32** (2010), 339–383.

[23] Mirebeau, J.M.: Optimally adapted meshes for finite elements of arbitrary order and $W^{1,p}$ norms. Numer. Math. **120** (2012), 271–305.

[24] Schwab, C.: *p- and hp-Finite Element Methods*. Clarendon Press, Oxford, 1998.

[25] Šolín, P.: *Partial Differential Equations and the Finite Element Method*. Pure and Applied Mathematics, Wiley-Interscience, New York, 2004.

[26] Šolín, P. and Demkowicz, L.: Goal-oriented *hp*-adaptivity for elliptic problems. Comput. Methods Appl. Mech. Engrg. **193** (2004), 449–468.

[27] Sun, S.: *Discontinuous Galerkin methods for reactive transport in porous media*. Ph.D. thesis, The University of Texas, Austin, 2003.

[28] Vejchodský, T., Šolín, P., and Zítka, M.: Modular *hp*-FEM system HERMES and its application to Maxwell's equations. Math. Comput. Simulation **76** (2007), 223–228.

[29] Zienkiewicz, O.C. and Wu, J.: Automatic directional refinement in adaptive analysis of compressible flows. Int. J. Numer. Methods Engrg. **37** (1994), 2189–2210.

Authors' addresses: *Vít Dolejší*, Charles University Prague, Faculty of Mathematics and Physics, Sokolovská 83, 186 75 Prague, Czech Republic e-mail: `dolejsi@karlin.mff.cuni.cz`.